コンクリート工学年次論文報告集, Vol.14, No.2, 1992

論 文

[2179] Cyclic Behavior of Concrete Based on Micromechanics

Ahmed M. FARAHAT *, *Zhishen WU* * and *Tada-aki TANABE* *

1. INTRODUCTION

In recent years, a large variety of models has been proposed to predict the behavior of concrete. Most of these models are based on the theory of plasticity. However, the classical approach of plasticity, with scalar loading function in order to satisfy the invariance conditions, becomes rather complex. Alternatively, an approach (called microscopic approach) based on the local view of the material properties can be adopted.

In the current study, the micromechanical model, originally introduced by the authors for the description of the monotonic behavior of concrete[2], is extended to predict the cyclic behavior of concrete. The microcracking, which is the most relevant cause of nonlinearity, is assumed to be localized in the thin and thick mortar layers. For this purpose, concrete is idealized to have two kinds of contacts; aggregate-aggregate and aggregate-mortar contacts. The behavior of these contacts is examined and distinguished for both cyclic and virgin loading. Finally an explicit formula which expresses the tangent stiffness matrix of the material as a summation of the contributions of all contacts, inside any representative volume, is derived. The proposed model is in contrast to the Bazant's microplane model[1], in which the microcracking was assumed to be localized only in the thin mortar layers and the concrete was idealized to have single kind of contact(aggregate-aggregate contact). Moreover, in that model[1], less attention was focused on the cyclic behavior. The proposed model has shown its capability to verify the test data.

2. THEORETICAL APPROACH OF THE PROPOSED MODEL

2.1 AVERAGE STRESS TENSOR BY AVERAGING CONTACT FORCES

In this study, concrete is idealized to have plural types of particles ; aggregate and mortar, and every mortar particle is assumed to be surrounded by a number of aggregate particles. As explained before[2], if there is a stress state σ_{ij}, which is in equilibrium but otherwise may be arbitrarily distributed in the region v, the average stress $\bar{\sigma}_{ij}$ is defined[2] as in eq.(1-a). Using the divergence theorem and the equilibrium condition, the average volume integral in eq.(1-a) can be reduced to the form in eq.(1-b).

* Department of Civil Engineering, Nagoya University

$$\bar{\sigma}_{ij} = \frac{1}{v}\int_v \sigma_{ij}dv \quad \text{.....(1-}a\text{)}, \qquad \bar{\sigma}_{ij} = \frac{1}{v}\sum_{m=1}^{n} f_i^m l_j^m \quad \text{.....(1-}b\text{)}$$

where n is the number of contacts per particle, both l_j and f_i are the contact vector and the contact force at the m^{th} contact. Now if eq.(1-b) is applied for both aggregate and mortar particles, the incremental mean stress for any volume can be obtained as follows:

$$\Delta\bar{\sigma}_{ij} = \frac{1}{V}\Big(\sum_{C_1}\Delta f_i^{C_1} l_j^{C_1} + \sum_{C_2}\Delta f_i^{C_2} l_j^{C_1} + \sum_{C_2}\Delta f_i^{C_2} l_j^{C_2}\Big) \tag{2}$$

where, C_1 and C_2 are the total number of contacts between aggregates alone and between aggregate and mortar particles while V is the total volume. If the contacts are grouped within a finite number of orientational intervals, the grouped average $\Delta\bar{f}\bar{l}(\theta)$ in eq.(2) can be calculated. For a large number of contacts and very small oriental intervals, eq.(2) can be written in an integral form[2].

2.2 AVERAGE CONTACT FORCES - STRAIN TENSOR RELATIONSHIP

Neglecting the possible rotation between particles, the average grouped contact force increments are linked with the displacement increments of the same group of orientation using the linear contact law as follows:

$$\Delta\bar{f}_n^c(\theta) = K_n\Delta\bar{\delta}_n^c(\theta), \qquad \Delta\bar{f}_s^c(\theta) = K_s\Delta\bar{\delta}_t^c(\theta) \tag{3}$$

where $\Delta\bar{\delta}_n^c(\theta)$ and $\Delta\bar{\delta}_t^c(\theta)$ are the relative normal and tangential displacement increments of the grouped contacts. K_n and K_s refer to the normal and shear stiffnesses of the contact, $\Delta\bar{f}_n^c(\theta)$ and $\Delta\bar{f}_s^c(\theta)$ are the components of contact force increments of the same group of orientations. Here, the normal and shear microstrains $(\varepsilon_n, \varepsilon_t)$ which govern progressive cracking and failure of microstructure, are assumed to be equal to the resolved components of macroscopic strains. It can be expected that the relative displacement increments taken over the contacts of similar orientations are as follow:

$$\Delta\bar{\delta}_n^{aa}(\theta) = \Delta\frac{\delta\bar{l}_n^{aa}(\theta)}{l} = K\,\Delta\bar{\varepsilon}_{ij}n_i n_j, \qquad \Delta\bar{\delta}_t^{aa}(\theta) = \Delta\frac{\delta\bar{l}_t^{aa}(\theta)}{l} = K\,\Delta\bar{\varepsilon}_{ij}t_i n_j \tag{4}$$

$$\Delta\bar{\delta}_n^{am}(\theta) = \Delta\frac{\delta\bar{l}_n^{am}(\theta)}{l} = \Delta\bar{\varepsilon}_{ij}n_i n_j, \qquad \Delta\bar{\delta}_t^{am}(\theta) = \Delta\frac{\delta\bar{l}_t^{am}(\theta)}{l} = \Delta\bar{\varepsilon}_{ij}t_i n_j \tag{5}$$

where (aa) and (am) refer to aggregate-aggregate and aggregate-mortar contacts. $\bar{\varepsilon}_{ij}$ is the average macroscopic strain, n and t are the direction cosines of the unit normal and the unit tangent of the contact. K represents the non-uniformity of strain distribution.

2.3 STRESS- STRAIN RELATIONSHIP

If the average normal and tangential contact forces increments in eq.(3) are combined with eqs.(4) and (5), and the resulting values are introduced into the integral form of eq.(2), the following incremental stress strain relationship can be obtained[2]:

$$\Delta\bar{\sigma}_{ij} = D_{ijkl}\,\Delta\bar{\varepsilon}_{kl} \tag{6}$$

where, $D_{ijkl} = \eta_1 \int_0^{2\pi} (k_n a_{ijkl} + k_s b_{ijkl})^{c_1} \bar{E}(\theta) K d\theta + \eta_2 \int_0^{2\pi} (k_n a_{ijkl} + k_s b_{ijkl})^{c_2} \bar{E}(\theta) d\theta$,

$\bar{E}(\theta) = 2\pi E(\theta) = 1 + A cos^2\theta - A sin^2\theta$, $a_{ijkl} = n_i n_j n_k n_l$, $b_{ijkl} = t_i n_j t_k n_l$,

$\eta_1 = C_1 \bar{l}_1 \bar{a}_1 / 2\pi V$, $\eta_2 = C_2 \bar{l}_1 \bar{a}_2 / 2\pi V + C_2 \bar{l}_2 \bar{a}_2 / 2\pi V$

$k_n = K_n / \bar{a} = d\sigma_n / d\varepsilon_n$, $k_s = K_s / \bar{a} = d\tau_{nt} / d\varepsilon_{nt}$

Both (c_1, $\bar{a}_1$) and (c_2, $\bar{a}_2$) refer to the contacts and the average contact areas between aggregate-aggregate and aggregate-mortar particles. $\bar{l}_1$ and $\bar{l}_2$ are the averages of the radii of aggregate and mortar particles. A is the non-homogeneity parameter. k_n and k_s are the normal and shear stiffnesses. In this study k_s is assumed to be linear with k_n (i.e. $k_s = \lambda k_n$). $E(\theta)$ is the density distribution function of the contact normals.

2.4 NORMAL STRESS-STRAIN RELATION OF THE CONTACTS

2.4.1 VIRGIN LOADING BEHAVIOR OF BOTH CONTACTS

Aggregate - Mortar Contact: The stress strain relation for the contact relating σ_n to ε_n, must describe the cracking and the damage all the way to complete fracture or failure, at which σ_n reduces to zero. It is clear that σ_n as a function of ε_n must first rise, then reach a maximum, and then gradually decline to zero. However eqs.(7-a) and (7-b) are proposed for the contacts in tension and in compression as shown in Fig.1-a,

$$\sigma_n^{am} = E_2 \varepsilon_n^{am} exp[-k_t (\frac{E_2}{E_1})^p (\varepsilon_n^{am})^p] ...(7-a), \qquad \sigma_n^{am} = E_2 \varepsilon_n^{am} exp[-k_c |\varepsilon_n^{am}|^{p_1}] ...(7-b)$$

where k_t, k_c ,p and p_1 are positive constants, E_1 and E_2 are the initial micro-stiffnesses of aggregate-aggregate and aggregate-mortar contacts, respectively.

Aggregate-Aggregate Contact: The normal stress-strain relationships proposed by Bazant[1] are used here. These relations are shown in eqs.(8-a) and (8-b) and in Fig.1-b.

$$\sigma_n^{aa} = E_1 \varepsilon_n^{aa} exp[-k_t (\varepsilon_n^{aa})^p] .....(8-a), \qquad \sigma_n^{aa} = -C_1 + C_2 tan^{-1}[C_3(\varepsilon_n - C_4)] .....(8-b)$$

where, $C_1 = -0.27 f_c'$, $C_2 = 0.87 f_c'$, $C_3 = 1.15(\frac{E_1}{f_c'})$, and $C_4 = -\frac{1}{C_3} tan\ (\frac{C_1}{C_2})$

2.4.2. CYCLIC LOADING

(1) Unloading path from tension

Aggregate - Mortar Contact: In the unloading from tension to compression, depending the coordinates of the reloading point in the previous cycle, either path (A) or path (B) will be followed as shown in Fig.1-a . Path (A), in which the compressive stress at the reloading point in the previous cycle is less than the microscopic peak stress, based on the experimental data, the following path is assumed:

$$\sigma_n = \sigma^* + \left[\frac{f_{to}}{3(\frac{\varepsilon^*}{\varepsilon_{tm}}) + 0.40}\right] \left[0.02 \left\{ ln\ (\frac{\varepsilon_n + \varepsilon_{rc}}{\varepsilon^* + \varepsilon_{rc}}) \right\}^5 - 0.80(\frac{\varepsilon_{tm}}{\varepsilon^*}) \sqrt{\frac{\varepsilon^* - \varepsilon_n}{\varepsilon^* + \varepsilon_{rc}}} \right] \qquad (9)$$

where ε^* and σ^* are the coordinates of the unloading point. Beyond the microscopic peak stress, the path in the next form will be followed:

$$\sigma_n = \left[\frac{1.86 + 15.0 * 10^5 (\varepsilon^*)^{2.5}}{1.00 + 15.0 * 10^5 (\varepsilon^*)^{2.5}} (0.538 f_{co})\right] \left[1 - (\frac{\varepsilon_{cc} - \varepsilon_n}{\varepsilon_{cc} - \varepsilon_{cm}})^2\right] \quad (10)$$

Path (B) in which the compressive stress at the reloading point in the previous cycle exceeded the microscopic peak compressive strength, is assumed to be as follows:

$$\sigma_n = \sigma^* + (\sigma_r - \sigma^*) \left\{\frac{\varepsilon_n - \varepsilon^*}{\varepsilon_r - \varepsilon^*}\right\}^{0.70}, \qquad \varepsilon_r = \varepsilon^* + 0.02\varepsilon^{**} \left\{ln(1 + 3.0(\frac{\varepsilon^{**} - \varepsilon_*}{\varepsilon_{oc}}))\right\} \quad (11)$$

where, ε^{**} is the coordinate of the reloading point in the previous cycle.

Aggregate - Aggregate Contact: As proposed by Bazant[1], eq.8(b) will be used if the unloading in tension takes place as shown in Fig.1-b. In eq.8(b) the expressions of C_1, C_2, C_3 and C_4 will be changed. More details are in ref.[1]

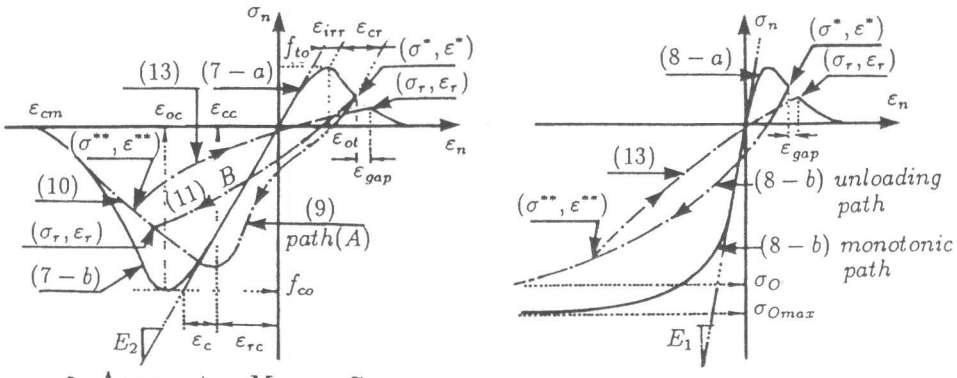

a- Aggregate - Mortar Contact b- Aggregate - Aggregate Contact

Fig.1 Normal Stress - Strain Relationship at Both Contacts

(2) Reloading path to tension

For both aggregate-aggregate and aggregate-mortar contacts, the gap in the envelope curve is described in eq.(12-a). The coordinate of the returning points on the envelope curve $(\sigma_r, \varepsilon_r)$ can now be obtained using eqs.(12-b), (7-a) and (8-a)

$$\varepsilon_{gap} = 0.02 \left\{ln(1 + 3.0(\frac{\varepsilon^* - \varepsilon^{**}}{\varepsilon_{ot}}))\right\} \text{.....}(12-a), \qquad \varepsilon_r = \varepsilon^* + \varepsilon_{gap} \text{.....}(12-b)$$

Starting from the reloading point $(\sigma^{**}, \varepsilon^{**})$ up to the reloading point $(\sigma_r, \varepsilon_r)$ at the envelope curve as shown in Fig. 1, the reloading curve is assumed to be as follows:

$$\sigma_n = \sigma^{**} + (\sigma_r - \sigma^{**}) \left\{\frac{\varepsilon_n - \varepsilon^{**}}{\varepsilon_r - \varepsilon^{**}}\right\}^{0.60} \quad (13)$$

(3) Unloading path from compression

The coordinates of the intersection point between the unloading curves and the strain axis are observed and modified to be suitable for microscopic path. Starting from the unloading point $(\sigma^*, \varepsilon^*)$ and passing through the modified point $(0, \varepsilon_A)$ up to the maximum tensile strength $(f_{to}, \varepsilon_{tt})$ as shown in Fig.1, the unloading curve in eq.(14-a) is assumed. Beyond the point of the maximum tensile strength eq.(14-b) will be followed.

$$\sigma_n = \sigma^* - \sigma^* \left\{ \frac{\varepsilon_n - \varepsilon^*}{\varepsilon_A - \varepsilon^*} \right\}^{0.60} \quad \text{.....(14-}a\text{)}, \qquad \sigma_n = f_{to} - f_{to} \left\{ \frac{\varepsilon_n - \varepsilon_{tt}}{\varepsilon_{tm} - \varepsilon_{tt}} \right\}^2 \quad \text{.....(14-}b\text{)}$$

$$\varepsilon_A(am) = \left[1 + 0.2(ln \left\{ \frac{\varepsilon_{cm}}{\varepsilon^*} \right\}) \right] \left[\frac{\varepsilon^* - (\sigma^*/E_2)}{1 + (\sigma^*/f_{co})} \right], \qquad \varepsilon_A(aa) = \frac{\varepsilon^* - (\sigma^*/E_1)}{0.70\ (1 + (\sigma^*/\sigma_{Omax}))}$$

(4) Reloading path to compression

For aggregate-aggregate and aggregate-mortar contacts, the gap in the envelop curve is described in eq.(15-a). The coordinates of the returning points on the envelope curve $(\sigma_r, \varepsilon_r)$ can be obtained by eqs.(15-b), (7-b), and (8-b)

$$\varepsilon_{gap} = 0.02 \left\{ ln(1 + 3.0(\frac{\varepsilon^* - \varepsilon^{**}}{\varepsilon_{oc}})) \right\} \quad \text{.....(15-}a\text{)}, \qquad \varepsilon_r = \varepsilon^* + \varepsilon_{gap} \quad \text{.....(15-}b\text{)}$$

Starting from the reloading point $(\sigma^{**}, \varepsilon^{**})$ up to the point $(\sigma_r, \varepsilon_r)$ at the envelope curve as shown in Fig.2, the reloading curve is assumed to be as follows:

$$\sigma_n = \sigma^{**} + (\sigma_r - \sigma^{**}) \left\{ \frac{\varepsilon_n - \varepsilon^{**}}{\varepsilon_r - \varepsilon^{**}} \right\}^{0.60} \qquad (16)$$

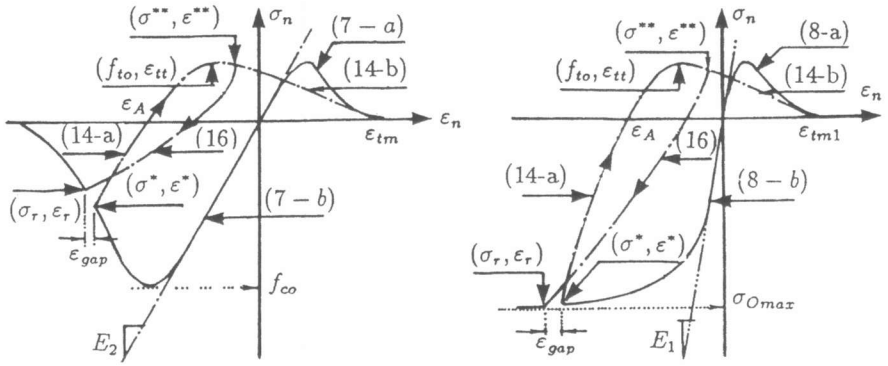

a- Aggregate - Mortar Contact b- Aggregate - Aggregate Contact

Fig.2 Unloading Path from Compression and Reloading to Compression

3. VERIFICATION OF THE PROPOSED MODEL

In the beginning, reasonable values of the parameters, which describe the characteristic properties of the contacts, are selected as follows; p=1.5, p_1=1.5(eq.7) and λ=0.20, η_1/η_2=0.05, $\eta_1 + \eta_2 = 1$[2], E_1/E_2=1.80, A=0.05 and K=0.80(eq.6). Finally, only k_t and k_c in eqs.(7-a), (7-b) and (8-a) are considered to be variable parameters. A sample of the results is shown in Fig.3. From Fig.3, satisfactory agreement is obtained. In the case of uniaxial tension, the value of k_c=50x10^4 is kept constant and the values of k_t= 51.5x10^4 and 78x10^4 are used for cases (a) and (b), while in uniaxial compression the value of k_t=30x10^4 is kept constant and the values of k_c=30x10^4 and 58x10^4 are used for cases (a) and (b), respectively. In uniaxial tension, the values of $10^{-4}E_1$ for cases (a) and (b) are 16.0 and 25.1 and those of $10^{-4}E_2$ are 8.89 and 14.39. In uniaxial compression, for cases (a) and (b), the values of $10^{-4}E_1$ are 14.8 and 23.23 and those of $10^{-4}E_2$ are 8.2

and 12.9, respectively.(All units of E_1 and E_2 are in kgf/cm^2)

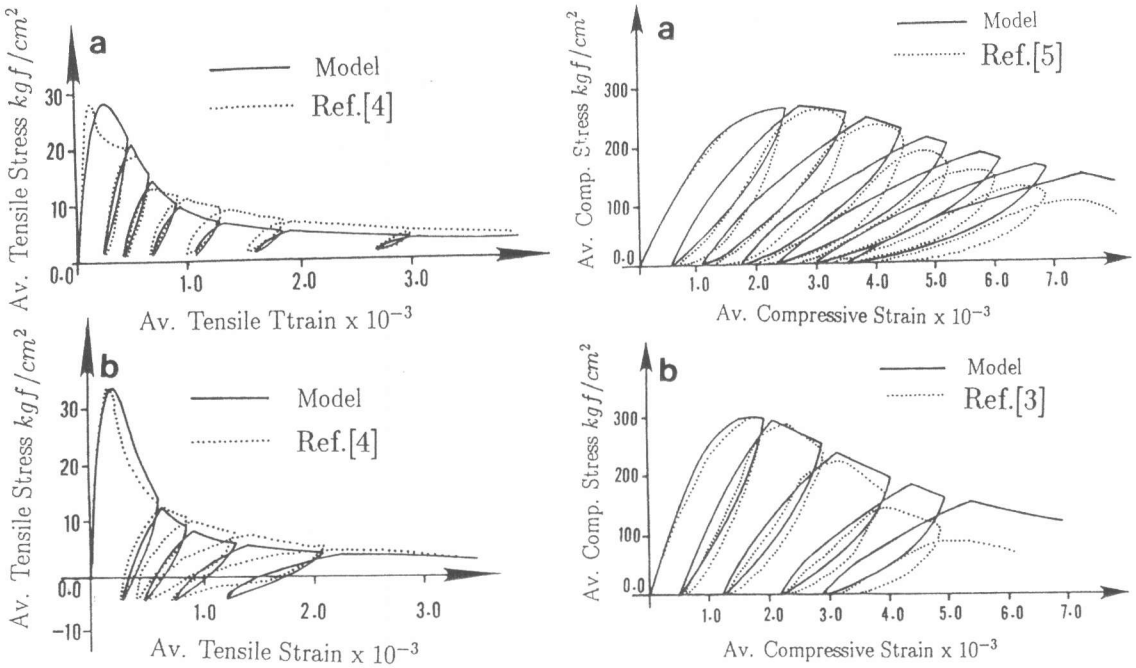

a- Uniaxial Tension b- Uniaxial Compression

Fig.3 Comparison with the Experimental Data

4. CONCLUSIONS

In the present study, the cyclic behavior of concrete is investigated through a new microscopic model. A reasonable agreement with the available macroscopic test data is obtained. This shows that the present model is capable of predicting the cyclic behavior of concrete. Also, to have more general understanding of the concrete, a comprehensive experimental work must be conducted not only on the macrolevel but also on the microlevel but with emphasis on the study on the more precise distribution of the contacts and also the strain distribution of the contacts.

REFERENCES

1. Bazant, Z. P. and Oh, A. M. ,"Microplane Model for Progressive Fracture of Concrete and Rock," Journal of Engineering Mechanics, ASCE , Vol. 111, No. 4, April 1985, pp. 559-582.

2. Farahat, A. M., Wu, Z. S. and Tanabe, T. ,"Development of Microplane Model of Concrete with Plural Types of Granular Particles," Proceeding of JSCE, 1991-08, No. 433, Vol. 15, pp. 231-238.

3. Okamoto, S., Shiomi, S., and Yamabe, K. ,"Earthquake Resistance of Prestressed Concrete Structures," Proceedings, Annual Convention, AIJ, 1976, pp. 1251-1952

4. Yankelevesky, D. Z., and Reinhardt, H. W. ,"Uniaxial Behavior of Concrete in Cyclic Tension," Journal of Structural Engineering, ASCE, Vol. 115, No. 1, Jan. 1989, pp. 166-182.

5. Sinha, B. P., Gerstle, K. H., and Tulin, L. G. ,"Stress-Strain Relations for Concrete Under Cyclic Loadings," Journal of American Concrete Institute, ACI, Vol. 61, No. 2, 1964, pp. 195-211.